Journal of Molecular Liquids 340 (2021) 117164

Contents lists available at ScienceDirect

Journal of Molecular Liquids

journal homepage: www.elsevier.com/locate/molliq

Strange behaviour of transport properties in novel metal thiocyanate based ionic liquids

Oscar Cabeza [a,*], Luisa Segade [a], Montserrat Domínguez-Pérez [a], Esther Rilo [a], David Ausín [a], Julio A. Seijas [b], M. Pilar Vazquez-Tato [b], Vladimir Matleev [c], Alexandr Ievlev [c], Josefa Salgado [d], Luis M. Varela [d]

[a] Departamento de Física y Ciencias de la Tierra, Facultade de Ciencias, Universidade da Coruña, Campus de A Zapateira s/n, E-15071 A Coruña. Spain
[b] Departamento de Química Orgánica, Facultad de Ciencias, Universidade de Santiago de Compostela, Rúa Alfonso X o Sabio s/n, E-27002 Lugo, Spain
[c] Department of Nuclear Physics Research Methods, Saint Petersburg State University, 78 199034, 7/9, Universitetskaya nab, Saint Petersburg, Russia
[d] Grupo de Nanomateriales, Fotónica y Materia Blanda, Departamento de Física de Partículas, Facultade de Física, Universidade de Santiago de Compostela, Campus Vida s/n, E-15782 Santiago de Compostela, Spain

ARTICLE INFO

Article history:
Received 29 September 2020
Revised 24 July 2021
Accepted 30 July 2021
Available online 03 August 2021

Keywords:
Thiocyanate ionic liquids
Ionic conductivity
Viscosity
Diffusion coefficient

ABSTRACT

In a previous paper some of us presented the structure and some properties of a new family of ionic liquids, ILs, with a common cation, 1-butyl-3-methyl imidazolium (the popular $[C4C1Im]^+$ or $[BMIM]^+$) and a variety of anions based in thiocyanate $(SCN)^-$: one reference sample and ten with anionic metal complexes of different valences: Al^{III}, Mn^{II}, Fe^{III}, Cr^{III}, Ni^{II}, Hg^{II}, Zn^{II}, Co^{II} and Cu^{I}, resulting, respectively, [BMIM](SCN), $[BMIM]_3$ $Al(SCN)_6$, $[BMIM]_4$ $Mn(SCN)_6$, $[BMIM]_3$ $Fe(SCN)_6$, $[BMIM]_3$ $Cr(SCN)_6$, $[BMIM]_4$ $Ni(SCN)_6$, $[BMIM]_2$ $Hg(SCN)_4$, $[BMIM]_2$ $Zn(SCN)_4$, $[BMIM]_2$ $Co(SCN)_4$ and $[BMIM]_3$ $Cu(SCN)_4$. In this paper we show experimental measurements of electrical conductivity of these ILs in a broad temperature range (about 90 K). Viscosity has been measured for six compounds in a wide temperature range. In addition, the diffusion coefficient for both ions forming the IL has been measured for some of the samples using NMR-Dosy technique. In spite of being very similar compounds from a chemical point of view, they present very different transport property values. Thus, viscosity varies more than two orders of magnitude among those metal thiocyanate ILs, being the highest for the compound with Al and the lowest for that with Hg. Moreover, differences between ionic conductivity and diffusion coefficient values extend more than one order of magnitude among the thiocyanate ILs. These three properties will be related in pairs, thus through Walden's rule we compare molar conductivity and fluidity, while using Kohlrausch's law and Nerst-Einstein equation molar conductivity and diffusion coefficient are related. Also, diffusion coefficient and fluidity (the inverse of viscosity) are compared by means of Stokes-Einstein relationship. In addition, we calculate the Laity interionic friction coefficients for both anions of the IL with Hg. Finally, a theoretical model is suggested to explain all the experimental evidences reported.

1. Introduction

In a recent paper some of us reported the synthesis and characterization of the different ionic liquids (ILs) studied here [1]. These ten compounds are all composed by the 1-butyl-3-methyl imidazolium cation and one thiocyanate based anion: [BMIM](SCN), $[BMIM]_3$ $Al(SCN)_6$, $[BMIM]_4$ $Mn(SCN)_6$, $[BMIM]_3$ $Fe(SCN)_6$, $[BMIM]_3$ $Cr(SCN)_6$, $[BMIM]_4$ $Ni(SCN)_6$, $[BMIM]_2$ $Hg(SCN)_4$, $[BMIM]_2$ $Zn(SCN)_4$, $[BMIM]_2$ $Co(SCN)_4$ and $[BMIM]_3$ $Cu(SCN)_4$. Chemical characterization was made by means of nuclear magnetic resonance (NMR), mass spectroscopy (MS-ES) and elemental analysis, Fourier transformed infrared (FTIR), Raman, optical, magnetic and thermal characterization, and also volumetric properties were measured. Different members of this family of ILs, based on thiocyanates, have been proposed for many interesting applications as electrolyte for supercapacitors [2] and batteries (mixed with lithium salts) [3], liquid fuel desulfuration [4], or toluene extraction [5]. This is because this family of ILs presents the common physicochemical properties of all ILs, including very low volatility, good electrical conductivity, broad electrochemical window, high stability both thermal and electrical [6,7]. In addition, they present interesting particular characteristics as no hygroscopicity, among the highest electrical conductivity and very high fluidity, and broad range of solubility for inorganic salts with common anion [3,8,9].

In this paper we report experimental measurements of some transport properties of these novel ILs, mainly their electrical conductivities, viscosities and diffusion coefficients. There are no pre-

* Corresponding author.
E-mail address: oscar.cabeza@udc.es (O. Cabeza).

https://doi.org/10.1016/j.molliq.2021.117164
0167-7322/

vious published data on these compounds except for the reference compound, the [BMIM](SCN) (which is a commercial IL). Viscosity of this IL, here used as reference, has been studied in many papers, both pure [9–11] and forming part of mixtures with different cosolvents, as water [12], alcohols [13,14], benzene or thiophene [15]. Even, its mixture with other [BMIM] based ILs has been studied [16]. In contrast, we have found only one paper where measurement of electrical conductivity in this IL appears [11], and no paper reports diffusion coefficient of any of the ILs shown here. It is important to note that the potential parameters for [BMIM](SCN) have been published, which are necessary to perform molecular simulations on this compound [17].

As reported in Ref. [1], we prepared metallic compounds based in [BMIM](SCN) and we obtained new ILs, which have very different physico-chemical properties. The metal cation generates anionic complexes with the thiocyanate anion, classified as adducts. Their morphology depends on the size and electronic structure of the metal cation, being the formed complex either in octahedral or in tetrahedral configurations for the metals used here. To the best of our knowledge, there is only one commercial metal thiocyanate, $[BMIM]_2$ $Co(SCN)_4$, which exhibits interesting properties as thermochromism [18,19], and it has been also proposed as electrolyte for dye-sensitized solar cells [20]. Very recently some of us reported the thermochromism that shows one of the ILs studied here, the $[BMIM]_4$ $Ni(SCN)_6$ [21]. Besides, novel metal thiocyanates with zinc and cadmium based in methyl imidazole have been published recently and their structure solved by single crystal X-ray diffraction [22], which exhibit luminescence properties. Finally, optical properties of some of these compounds, those containing Co, Zn, Ni or Cu, have been published by some of us [23]. Definitively, these ILs based in metal thiocyanates are very promising materials with many potential applications in fields as electrochemistry, photonics or catalysis.

Knowledge of transport properties is crucial to develop any real application and both electrical conductivity and viscosity are two of the most demanded data. The fact that so similar compounds give so different transport property values is a challenge to understand the charge and mass transport mechanisms in these compounds. Based on the diffusion coefficient measurements of both ions a model to explain the transport mechanism phenomena is proposed.

Finally, note that parent compounds based in cyanate anion (but not ionic liquids) have negative thermal expansion coefficient [24,25], but this effect has not been observed in the metal thiocyanate ILs studied in this paper.

2. Experimental details

2.1. Compounds

All the chemicals studied were synthesized by us, except [BMIM](SCN) and $[BMIM]_2$ $Co(SCN)_4$, which were purchased to IOLITEC with, respectively, a purity higher than 98% and 99% reported by de dealer. The other compounds have been characterized by NMR, electrospray ionization and MS-ES, which allows the determination of their purities, higher than 95% for all compounds [1]. Reference sample contains a water quantity of 4600 ppm from Karl-Fisher titration, while the other compounds (except that with Hg) have only traces [1]. Then, compounds have been analysed using FTIR and Raman spectroscopy. In addition, magnetic susceptibility and refractive index measurements were performed in some of the compounds studied, as well as thermal characterization using differential calorimetry, DSC, and thermal gravimetry, TGA. Finally, experimental measurements of density on all ILs have been performed, and for some of the samples in a broad temperature range (about 100 K). All these data have been originally reported in Ref. [1]. In Fig. 1 we show a schematic representation at scale of two metal-thiocyanate complex anions with octahedral (at left) and tetrahedral (at right) configurations and that of the [BMIM] cation (in the centre of Fig. 1).

2.2. Experimental techniques

2.2.1. Ionic conductivity

Ionic (or electrical) conductivity (κ) was measured using a CRISON GLP31 conductivimeter, which employs an ac voltage of 500 Hz and 0.50 Vrms, being the constant cell used $C \approx 1\ cm^{-1}$, and the distance between electrodes 3.5 mm. Capacity effect has been evaluated and it is below the reproducibility of the measured value. Calibration was made weekly with two certified KCl solutions with different concentration to cover the range of values measured. All measurements were performed using the isothermal method: the sample was immersed into a Julabo F25 thermostatic bath which controlled the temperature with an uncertainty of ±0.1 °C, it was tempered for at least 15 min at each single temperature before measuring it three consecutive times. The experimental relative uncertainties are less than a 0.5% of the measured κ value, being the repeatability better than a 3%. Ionic conductivity has been measured for all samples in a broad temperature range, and a minimum of three no consecutive times at 25 °C (at the beginning, at the end and in the middle of the measurement process), being the three values within the given uncertainty in all data series shown here.

2.2.2. Dynamic viscosity

Dynamic viscosity (η) was measured with an Anton Paar Stabinger SVM 3000 viscodensimeter with a repeatability better than 0.4% of the value measured and a reproducibility about 1%. This device has an internal Peltier thermostat featuring an uncertainty of ±0.02 °C in the temperature range studied, from 5 °C to 95 °C. The apparatus is verified daily with ethanol, and every four months we use five standard fluids from Anton Paar to verify calibration in all range of viscosity. The main advantage respecting other viscometers is that this one allows the measurement of viscosities from 0.2 to 20,000 mPa·s without changing any instrumental part, and so it is the most adequate apparatus to measure these samples because differences of some orders of magnitude appear among their viscosity values, and more than 20 times in each compound in the temperature range used. Viscosity was measured for six selected samples, the reference one and those with Al, Zn, Hg, Cu and Cr anionic complexes, following the isothermal method described above. The other samples have not been measured due to their very high viscosity at room temperature or for being chemically incompatible with the viscodensimeter materials. In spite of the fact that Stabinger uses a magnetic field to perform the measurement, we have not observed any anomalous behaviour of the values obtained for sample with Cr (the only magnetic nucleus measured). To be sure, we have measured the viscosity of this same sample with a rolling ball viscosimeter at room temperature, and results agree with those published here within experimental uncertainties.

2.2.3. Diffusion coefficient

The diffusion coefficients (D) of the anion and the cation were measured using the well-known pulsed field gradient (PFG) NMR technique on ^{13}C and ^{1}H nuclei. Bruker Avance III WB 400 MHz NMR spectrometer was used with the standard *diffSte* pulse sequence. The measurements were performed in the MR Center of the Research Park of Saint-Petersburg State University. The maximum strength of the used pulse gradient was 30 T/m. The pulses duration and the interval between them were chosen as 1 ms and

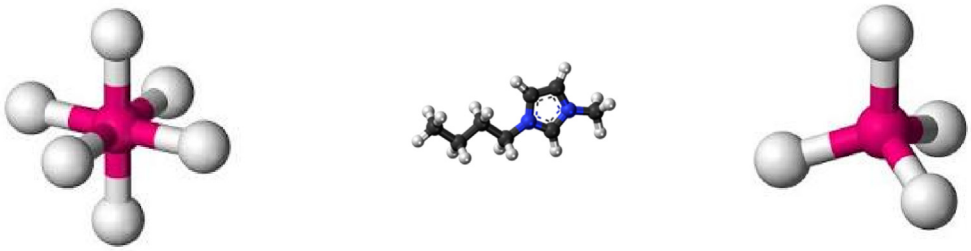

Fig. 1. Size scaled scheme of the three anion types studied: Two metal thiocyanate anionic complex, in octahedral (at left) and tetrahedral (at right) configurations. Red balls represent the metal cation while white ones (SCN) anions. In the middle, size scaled scheme of the [BMIM] cation, where white balls are for H, black for C and blue for N atoms.

100 ms, respectively. All measurements were carried out at a stabilized temperature in the entire volume of the sample, with a stabilization precision of 0.1 °C. The total relative uncertainty of the calculated diffusion coefficients, including the repeatability of the experiment, was not more than 6% for ^{13}C nuclei and not more than 2% for ^{1}H ones, respectively. We have measured the ion diffusivity of the [BMIM](SCN) reference sample and of those with Zn, Cu, Al or Hg at 25 °C. For two last ones the D values were also measured in a broad temperature range (from 273 K to 363 K). We did not measure D for the samples with paramagnetic metals, namely, Co, Ni, Mn, Fe, and Cr, because in this case both ^{1}H and ^{13}C relaxation times are too short to realize the PFG approach.

3. Results

In this section we summarize the results obtained for the three properties measured: ionic conductivity, dynamic viscosity and diffusion coefficient. Also, we have calculated molecular conductance from the experimental values presented here and in Ref. [1]. So, we have divided this section into four subsections devoted to each one of the four properties analysed. All results contained here have not been previously published for any studied IL, except for [BMIM](SCN), which is considered here as a reference or base IL. Ionic conductivity for this compound has been reported, up to our knowledge, only once [11], being the values reported about 10% smaller than the ones measured here, probably due to different water content of the samples. In contrast, viscosity of [BMIM](SCN) has been measured by many groups, and we have found 9 references giving those data in the temperature range studied here. Some of the results are less than 2% higher to ours [10–14], while others are higher than 5% [5,9,15], and even 25% higher [16]. Again, differences in water content and in other impurities of the samples could be the reason of the differences observed. It is necessary to take into account that our reference compound had not been dried, and it was used as received from the supplier (with 4600 ppm of water as written above). Only before NMR measurements, all samples were dried to a more accurate diffusion constant measurement.

Temperature dependence of all transport properties measured can be fitted with high precision with a Vogel-Tamman-Fulcher (VTF) type equation [26–28].

$$Y = Y_\infty exp\left\{\frac{B_Y}{T - T_Y}\right\} \tag{1}$$

where Y is a transport property (electrical conductivity, viscosity, molar conductivity, diffusion or friction coefficients), and Y_∞, B_Y and T_Y are considered here as fitting parameters. Although they have a physical meaning in the original formulation, comparison among them in different compounds and properties is difficult, and contradictions appear in the interpretation of each constant for every property [29]. For example, T_Y is called Vogel temperature, at which the ions is supposed to lose their mobility completely. In this case, its value would be very similar for a given compound, independently of the property fitted. But this is not the case, and differences of up to 40 K appear among the samples studied here as we will see later.

The temperature behaviour of the four transport properties for all compounds can also be fitted using Litovitz's equation [30,31], which reads

$$Y = Y_L exp\left\{\frac{B_Y^L}{T^3}\right\} \tag{2}$$

where Y_L and B_Y^L are fitting parameters. As it happens with the VTF equation, it has been given a physical meaning to these two parameters, but conclusions obtained for the different ILs and properties measured are noncoherent as it will be observed below.

In the temperature range measured both equations fit very well the experimental data, and if we plot VTF and Litovitz equations in a figure, both curves would match and it would not be easily distinguishable by naked eye.

It is important to note that the minimizing factor in the fitting processes was not the usual standard deviation, s, but the percentage standard deviation, $s\%$. This last magnitude is defined as,

$$s\% = 100\sqrt{\frac{\sum_{i=1}^{N}\left[\left(Y_{exp,i} - Y_{theo,i}\right)/Y_{exp,i}\right]^2}{N-1}} \tag{3}$$

where $Y_{exp,i}$ is the value measured of the corresponding transport property at a given temperature, $Y_{theo,i}$ that obtained from the VTF or Litovitz equations, and N the number of data points used for the fitting (all measured ones with the sample in liquid state). We have used $s\%$, instead of the most common standard deviation, due to the high variation of the Y value with temperature in all samples and properties. Thus, while $s\%$ gives a similar weight in the fitting for all data points, s gives more weight to those with highest values.

3.1. Ionic conductivity

We have measured the ionic conductivity of the ten studied compounds in a wide temperature range, from 5 °C to 95 °C for most of them. Results are plotted in Fig. 2 while the data appear in Table S1 of Supporting Information. As expected, the highest measured ionic conductivity corresponds to the reference sample, while those with tetrahedral coordination (Hg, Zn, Cu and Co) present higher values (in that order) than those with octahedral one (Mn, Fe, Ni, Cr and Al in order decreasing to its κ value). The κ values measured range from 18 to 31 mS/cm at 95 °C among the samples with the first mentioned configuration, and from 5 to 19 mS/cm for those with the octahedral one, being quite similar for the samples with Co and Mn at T > 65 °C (in spite of the different configuration). Moreover, we can observe a trend of the ionic conduc-

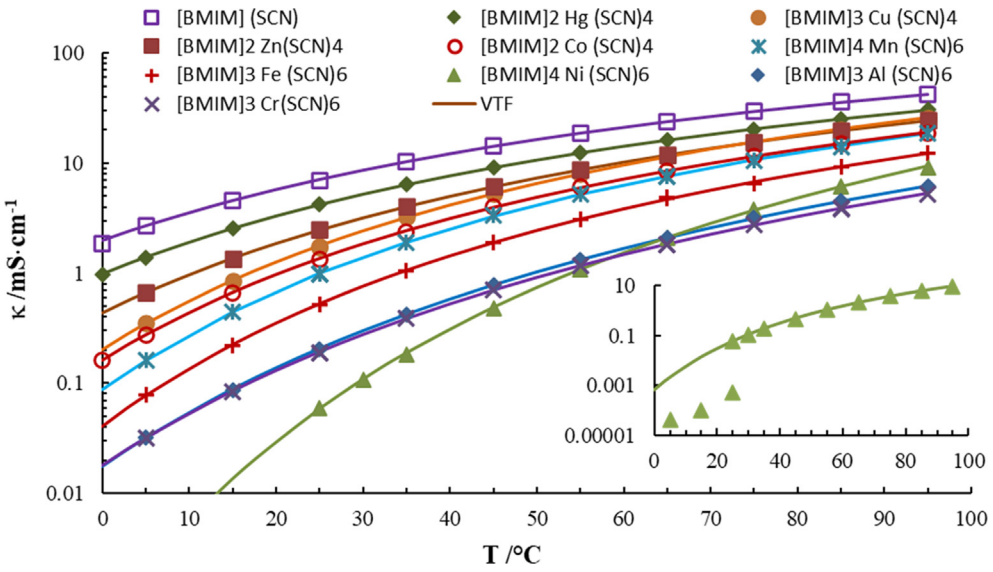

Fig. 2. Ionic conductivity for the ten studied thiocyanate ILs versus temperature in a semi-logarithmic plot. Curves are the best fit of VTF-type equation (1) with the fitting parameters given in Table 1. The inset shows conductivity of the Ni based IL to magnify the solidification process upon cooling the sample.

tivity with the electronic configuration of the metal, related itself with the ionic complex stability. Thus, the order of κ values at room temperature for the different thiocyanate metals is: Hg > Zn > Cu > Co > Mn > Fe > Cr > Al > Ni; which corresponds with the first row of transition metals, except for the magnetic nuclei (Fe and Ni) and Al. The compound with Ni has the highest melting point, and so a sudden jump in its conductivity value is seen at the solidification temperature, as shown in the inset of Fig. 2.

The temperature behaviour does not follow a simple Arrhenius relationship, but data fits very good to VTF and Litovitz Eqs. (1) and (2), respectively, as has been verified for many other ILs [32–34]. The best fit of VTF type Eq. (1) for each sample is shown in Fig. 2 as continuous lines. In Figure S1 of supporting information, we show a Litovitz representation of our data with the best fitting curves plotted. The best fitting parameters obtained for both, VTF and Litovitz equations, are given in Table S2 in Supported Information. In addition, note that in liquid state the $[BMIM]_4$ $Ni(SCN)_6$ presents the lowest K value at low temperatures, but when warming its ionic conductivity is higher than those of the samples with Al or Cr. In Table 1 we have introduced some characteristics of the different metallic elements used to synthesise the new IL compound, including atomic mass, M_M, and metal ion radii, R_{ion} (from Ref. [35]). We include two additional parameters proportional to the voltage at the metal ion surface, U (=q/R_{ion}), and to its charge surface density, σ (=q/R_{ion}^2), being q the nuclei charge.

3.2. Molar conductivity

Density of all compounds studied here (except for the Ni thiocyanate that is solid at room temperature) have been reported previously [1]. All of them have a linear behaviour with temperature in the range studied, whose negative slope indicates a positive thermal expansion coefficient. The slope increases its absolute value with the increase of the density of the given IL. Analysing density data, we discovered that molar volumes of the thiocyanate metallic complexes are very similar among them for each complex configuration, being at 25 °C, about 200 cm^3 per mol for the tetrahedral one, and about 240 cm^3 per mol for the octahedral configuration. In contrast $[BMIM]^+$ cation size depends on the ionic environment, thus we calculated about 133 and 143 cm^3 per mole, respectively for each configuration given, while when it is free in a molecular solvent its molar volume is only 117 cm^3. Note that molar volume of the anionic complex increases with temperature. Finally, the molar volume of the $(SCN)^-$ ion is about 65 cm^3 per mol, constant in the temperature range studied [1,11,28].

To understand the charge transport mechanisms for all compounds measured it is better to work with molar conductivity, which gives information about the average charge carried out by one single mole of each compound. From density, ρ, and ionic conductivity, κ (obviously at the same temperature) we can calculate the molar conductivity, Λ, knowing the ionic concentration, C ($mol \cdot L^{-1}$), inverse of the molar volume, V_m, thus

Table 1
Metal atom mass, MM; metal ion radii (from Ref. [35]), Rion; electrical surface potential of metal ion, U; charge surface density in metal ion, σ (in electron charge with radio in Å); ionic conductivity (in $mS \cdot cm^{-1}$), κ, and molar conductivity (in $mS \cdot cm^2 \cdot mol^{-1}$), Λ; at 25 °C and 75 °C.

	MM/Da	Rion/Å	U (q/Rion)	σ (q/Rion^2)	κ (25 °C)	κ (75 °C)	Λ (25 °C)	Λ (75 °C)
[BMIM] (SCN)	–	–	–	–	6.99	29.9	1.298	5.675
$[BMIM]_2$ $Hg(SCN)_4$	200.59	0.960	2.08	2.17	4.23	20.2	1.955	9.599
$[BMIM]_2$ $Zn(SCN)_4$	65.38	0.600	3.33	5.56	2.47	15.5	1.172	7.572
$[BMIM]_3$ $Cu(SCN)_4$	63.55	0.600	1.67	2.78	1.74	15.5	1.044	9.580
$[BMIM]_2$ $Co(SCN)_4$	58.93	0.580	3.45	5.95	1.33	11.5	0.620	5.520
$[BMIM]_4$ $Ni(SCN)_6$	58.69	0.690	2.90	4.20	0.059	3.80	–	–
$[BMIM]_3$ $Fe(SCN)_6$	55.85	0.645	4.65	7.21	0.519	6.54	0.353	4.576
$[BMIM]_4$ $Mn(SCN)_6$	54.94	0.830	2.41	2.90	0.985	10.6	0.813	8.991
$[BMIM]_3$ $Cr(SCN)_6$	52.00	0.615	4.88	7.93	0.191	2.78	0.129	1.931
$[BMIM]_3$ $Al(SCN)_6$	26.98	0.535	5.61	10.5	0.204	3.16	0.138	2.191

$$\Lambda = \kappa/C = \kappa \cdot M/\rho = \kappa \cdot V_m \quad (4)$$

where M is the molar mass of each IL, and *Vm* is given in Ref. [1] for all compounds at different temperatures. The calculated molar conductivity data are plotted in Fig. 3, where we observe the exponential increase with temperature. In general, the tetrahedral compounds present higher molar conductivity than those with octahedral one, but there are exceptions. Thus, at 95 °C one of the highest values is for $[BMIM]_4$ $Mn(SCN)_6$, while one of the lowest values is for $[BMIM]_2$ $Co(SCN)_4$, very similar than Λ for $[BMIM]_3$ $Fe(SCN)_6$. Note also that the molar conductivity of the reference sample is very small compared with its very high ionic conductivity value. Again, we observe that the Λ values obtained do not show a clear trend with the metallic ionic radii, electrical charge, surface charge density or electrical potential of the metal ion given in Table 1 (where we include data for Λ at 25 °C and 75 °C for an easy comparation). Temperature dependence of this property follows also the VTF and Litovitz equations, as already published for other ionic liquids [31]. The corresponding curves obtained are shown in Fig. 3 for VTF and in Figure S2 for Litovitz plots, while the best fitting parameters for both models appear in Table S3.

3.3. Viscosity

Dynamic viscosity of four [BMIM] metal thiocyanates, those with Al, Cr, Hg or Zn, and that of the reference sample, have been measured covering a temperature range of 90 K (from 278 K to 368 K). Results are plotted in Fig. 4 while the data measured appear in Table S4 in Supporting Information. Viscosity value varies greatly between the two different adduct configurations, thus the two compounds with the octahedral configuration measured are more than 10 times more viscous than those with the tetrahedral one.

As expected, the reference sample has the lowest viscosity. Temperature dependence of viscosity follows a VTF relationship given in Eq. (1) and Litovitz equation (2). In fact, both models have been developed primarily for dynamic viscosity [26–28,30], while later both have been used to fit all the other transport properties for the majority of electrolytes, including ILs [29,31–34,36]. The best fitting parameters obtained for VTF in the six samples have not any correlation with the corresponding values obtained for κ or Λ, as observed in Table S5. In this case, the B_η values are much higher than the B_κ ones for all the samples, but not uniformly. Also, the value of T_η is up to 30 K lower than T_κ for some samples, but in some others both temperatures are similar. The same happens for Litovitz B_η^L best fitting parameters obtained. If they are compared with those obtained from K, given in Table S3, nor the values of B_κ^L in every compound, neither the order of them in the different ILs agree between both magnitudes.

3.4. Diffusion coefficient

Both $[BMIM]^+$ cation and $(SCN)^-$ anion diffusion coefficient, *D*, have been measured independently using ^{13}C nucleus, since carbon is a part of both the cation and anion. Unfortunately, some of the compounds cannot be studied with this technique due to the paramagnetic character of the metal, as it happens with five of our samples, namely those with Co, Ni, Mn, Fe, and Cr. Following the data obtained for all samples measured, we would like to emphasize that (i) only a single peak has been observed for each complex anion, which indicates that all ions of each kind are in the same chemical environment, and (ii) the amplitude line of anion has shown one-exponential decay as a function of square the magnetic field gradient, and this indicates that all anions diffuse equally. The *D* values for 25 °C collected on Table 2 demonstrate that the mobility of each $[M(SCN)_n]^{-y}$ anion in every compound studied is lower than the $[BMIM]^+$ cation one, while it is *vice versa* for the reference sample [BMIM](SCN). This fact agrees well with the cation and anion relative sizes given in [1] and has already been commented in Section 3.2. Great differences among D values of the same $[BMIM]^+$ cation in the different compounds are observed, which is unexpected taking into account that the cation is the same and the environment also similar, at least apparently. For the anionic complexes the data are also unexpected, while the anionic abduct size is similar for all the tetrahedral anions [1], its diffusion coefficient differs significantly among them.

For the two most representative compounds, $[BMIM]_3$ $Al(SCN)_6$ and $[BMIM]_2$ $Hg(SCN)_4$, the temperature dependence of the diffusion coefficient has been also measured, the cation *D* was measured using ^1H and ^{13}C nucleus, while the anionic complex obviously only with ^{13}C. The data obtained are shown in Table S6 for the cation, from ^1H NMR, and in Table S7 for both cation and anion, from ^{13}C NMR. Note that these two compounds show the extremal values, both for viscosity as for ionic conductivity, which do them good candidates to study and compare. In Fig. 5 we plot the temperature dependence of diffusion coefficient for the two

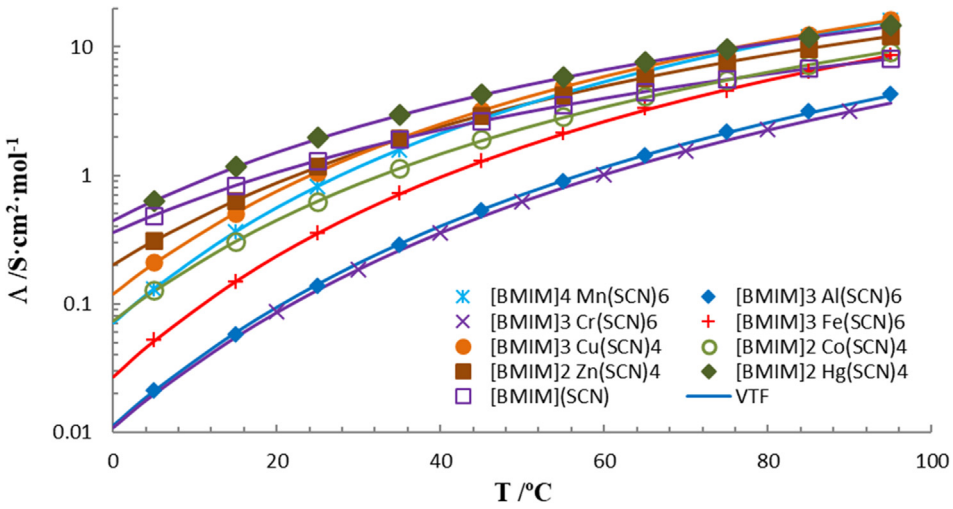

Fig. 3. Semi-Arrhenius plot of the molar conductivity of the reference sample and eight different [BMIM] metal thiocyanates studied (all except that with Ni) versus temperature with the VTF best fitting equations shown.

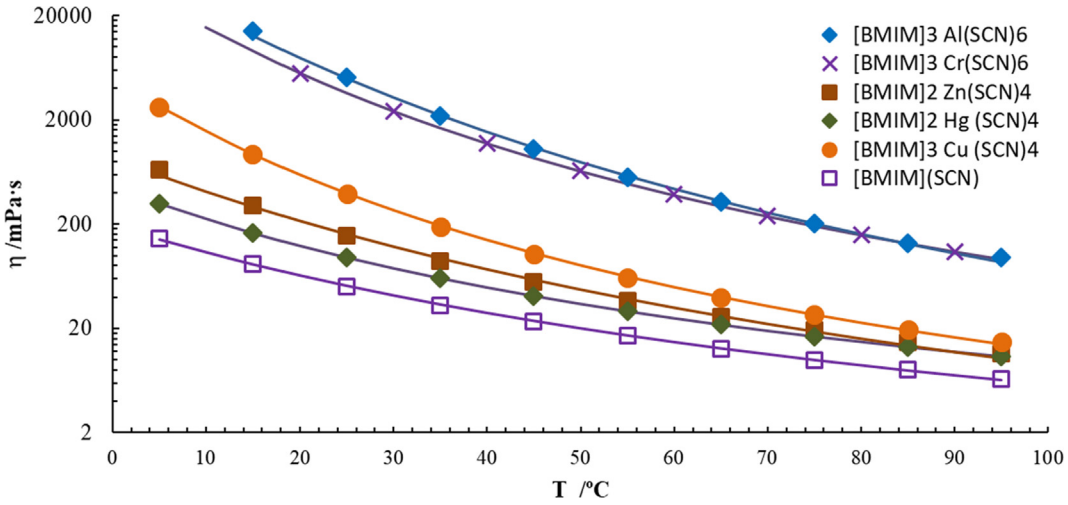

Fig. 4. Dynamic viscosity versus temperature for six thiocyanate based ILs. Semi-Arrhenius plot with the VTF best fitting curves shown for each sample.

Table 2
Diffusion coefficient for some of the of the cations, D_B, and metal adducts, D_M, at 25 °C, theoretical values of molar conductivity and diffusion, Λ_{NE} and D_{SE}, and deviation parameters, Δ_N and Δ_{SE} (see text for details).

Compound	$D\cdot10^{-12}$ m$^2\cdot$s^{-1}		Λ_{NE}	Δ_{NE}	D_{SE}	Δ_{SE}
	$[BMIM]^+$	$M(SCN)_n^-$	S·cm^2·mol^{-1}		10^{-12} m$^2\cdot$s^{-1}	
[BMIM] (SCN)	16.0	39	2.07	0.37	10.3	−0.10
$[BMIM]_2Hg(SCN)_4$	16.8	10.4	2.83	0.32	4.01	−0.16
$[BMIM]_2Zn(SCN)_4$	12.0	4.5	1.58	0.26	2.44	−0.05
$[BMIM]_3Cu(SCN)_4$	7.5	5.9	2.84	0.63	0.894	−0.96
$[BMIM]_3$ $Al(SCN)_6$	0.98	0.19	0.174	0.19	0.0665	−0.79

u(T) = 0.1 °C; u(D_B) < 2%, u(D_M) < 6%.

thiocyanate complex anions and [BMIM] cations for the two named ILs.

As expected, diffusion coefficients increase with temperature following also the VTF type Eq. (1) and the Litovitz equation (2) (but now with D instead Y). The best fitting curves are plotted in Fig. 5 for VTF and Figure S4 for Litovitz equation. Also, the best fitting parameters for the two analysed compounds and the two anions, appears in Table S8. As mentioned for the previous properties analysed, fitting parameters seems not to have any relationship with those obtained from the fittings of the previous transport magnitudes.

4. Discussion

In this section we analyse the experimental data obtained relating the three properties measured with classical physics-chemistry models. For that, we firstly compare molar conductivity with viscosity through Walden's rule. Then we relate molar conductivity

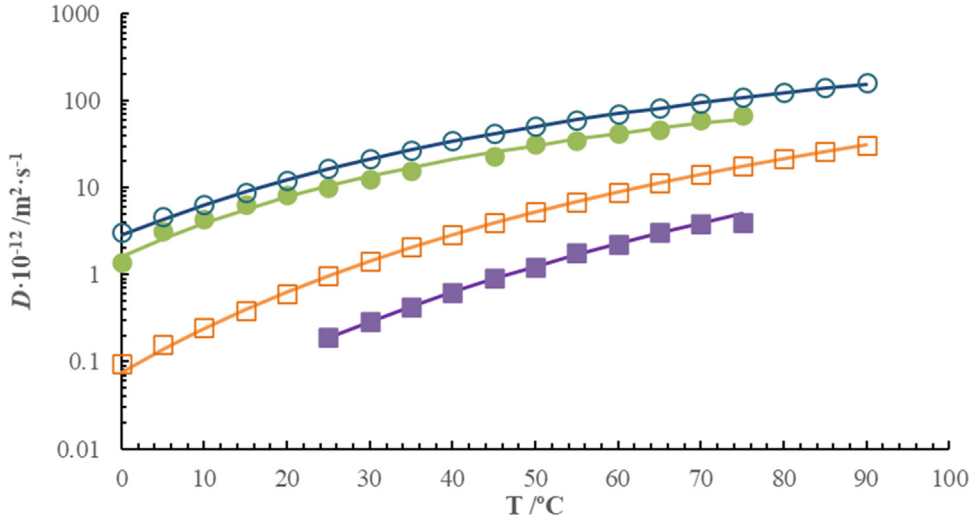

Fig. 5. Semi-Arrhenius plot of the diffusion coefficient versus temperature for the two thiocyanate complex anions (solid symbols), and the [BMIM] cations (open ones) for the ILs $[BMIM]_3$ $Al(SCN)_6$ (square symbols) and $[BMIM]_2$ $Hg(SCN)_4$ (dot ones). The VTF best fitting curves are plotted for each ion.

with diffusion coefficient using Nernst-Einstein equation, and finally, diffusion coefficient with fluidity (the inverse of viscosity) using the Stokes-Einstein equation. In addition, we calculate the interionic friction coefficient which gives information about the mobility of the different ions. From these comparisons we propose a theoretical model to explain all measured data and their relationships based on the microscopical structure of the different ILs studied.

4.1. Walden plot

To relate molar conductivity with viscosity we employ fractional Walden's rule [37–40],

$$\wedge \cdot \eta^{\gamma} = K; \quad \log\ \wedge(T) = \log K + \gamma \log\, \eta^{-1}(T) \tag{5}$$

The graphical representation of this equation is known as Walden's plot, where the slope γ is related with the ratio of activation energies of conductivity and fluidity [37]. Note that if in the VTF (or Litovitz) fittings we obtain $T_{\Lambda} = T_{\eta}$ and $B_{\Lambda} = -B_{\eta}$ (or $B^{L}_{\wedge} = -B^{L}_{\eta}$), then γ would or be equal to 1, and we will recover the original Walden's rule, usually followed by highly diluted electrolyte solutions [37]. Walden's plot takes as a reference the ideal line obtained from 0.01 M aqueous KCl solutions where log Λ (in S·cm^2·mol^{-1}) is equal to log η^{-1} (in Poise^{-1}) for all range of values. In this ideal solution ions are fully dissociated and both anion and cation have equal mobilities. The deviation of data obtained for any electrolyte from the reference line of KCl is an indicator of its "degree of ionicity" [37–40], although that comparison of ILs behaviour with that ideal reference line has been criticized [41], due to the very different environment of the ions in a dilute solution relative to that in highly concentrated media such ILs. In contrast, other authors, through molecular dynamic simulations, have verified the validity of Walden's plot (and Nerst-Einstein model) to relate viscosity and ionic conductivity [42]. In Fig. 6 we show Walden's plot for the six samples where viscosity have been measured. All compounds exhibit a linear behaviour with γ = 0.90 ± 0.04 for all except for the IL with Cu which presents the lowest value (γ = 0.83), the highest one is that for the IL with Hg (γ = 0.93), values typical of ILs [38–41]. Anyway, the linear relationship between molar conductivity and fluidity remains, which is an indication that temperature dependence of both properties is the same, as commented before. The most intriguing fact is that all metal thiocyanates appear as superionic, i.e., its corresponding line is above the ideal KCl line. This fact is not usual, but have been observed before in other systems involving ILs [34,43], suggesting that other mechanisms of charge transport appear in these ILs apart from the classical ionic diffusion.

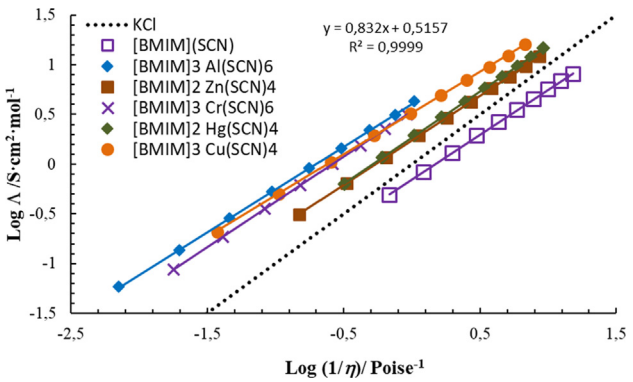

Fig. 6. Walden's plot of six studied IL compounds in an Arrhenius diagram of molar conductivity versus fluidity. Solid lines are the best fit of the corresponding series to a straight line, while dotted line represents ideal KCl solution.

4.2. Nernst-Einstein relation

Nernst-Einstein (NE) equation predicts that, in a diluted electrolyte, the molar conductivity, Λ_{NE}, is proportional to the diffusion coefficient through the equation [44], which has been used previously to analyse data from other ILs [42,45,46]

$$\Lambda_{NEi} = \frac{N_A}{k_B T} p_i q_i^2 D_i \tag{6}$$

where N_A is Avogadro's number, k_B is Boltzmann's constant, T is the absolute temperature, p_i is the number of ions i, q_i is the electrical charge of those anions and D_i is its diffusion coefficient. We have two type of ions in each compounds, named B and M respectively: cation $[BMIM]^+$, and metallic anionic complex $[M(SCN)n]^{-(n-z)}$ (where z is the metal cation valency, and n = 4 or 6 for, respectively, tetrahedral or octahedral configurations). Thus, in Eq. (6): i = A or M, $p_B = (n\text{-}z)$, $q_B = e$, $p_M = 1$, $q_B = (n\text{-}z)e$ (being e the electron charge). D_B and D_M are different for each compound, being the measured values given in Table 2 for five compounds at 25 °C, and in Table S7 for those with Hg and Al in a broad range of temperatures. Thus, following Kohlrausch's law, derived from Nerst-Einstein model, we can calculate the molar conductivity of the samples, by adding the contributions of the two ions

$$\Lambda_{NE} = \frac{N_A e^2}{k_B T}\left[(n-z)D_B + (n-z)^2 D_M\right] \tag{7}$$

We have calculated this theoretical Λ_{NE} using our measured values of D_B and D_M given in Table 2, where we have included the obtained Λ_{NE} values. Results obtained for the theoretical molar conductivity are higher than those experimentally measured, given in Table 2. This is usual for concentrated electrolytes, the NE equation was derived for noninteracting ions, as in an infinitely dilute electrolyte solution [44], where Eq. (7) is exact. Actually, mass, charge, momentum, and energy transport processes in ILs involve correlated collisions, caging, and vortex motions, as in any other dense electrolyte. Due to that, it has been defined the Nernst–Einstein deviation parameter Δ_{NE} [45–47],

$$\Lambda = \Lambda_{NE}(1 - \Delta_{NE}) \tag{8}$$

Δ_{NE} is related to differences in cross-correlations of ionic velocities and it is usually positive. Harris [45] has provided a clear treatment of the statistical mechanical basis for Δ_{NE}, and gives a summary of experimental values for a range of ionic liquids. He found that Δ_{NE} is typically a weak function of temperature and pressure, but does vary with the size and nature of the ions [48]. We have obtained the Δ_{NE} value for the compounds studied here at 25 °C, being the results summarized in Table 2. As observed, all values are positive, ranging from 0.19 for the sample with Al up to 0.63 for that with Cu. Note that Hg and Zn compounds presents a similar value of parameter Δ_{NE}, in accordance with Walden's plot, where both ILs show nearly identical curves. To observe the variation of Δ_{NE} with temperature, we use the D data from Table S7 to obtain Λ_{NE}. In Fig. 7 we show the molar conductivity data measured experimentally, Λ, and Λ_{NE} calculated with Eqs. (6)–(8) versus temperature. We have used in Eq. (8) the average value of Δ_{NE} at all temperatures, being higher than those for 25 °C (thus, we used Δ_{NE} = 0.30 for the IL with Hg and Δ_{NE} = 0.26 for that with Al). As observed in Fig. 7, the temperature dependence is the same for both sets of data in each sample, and the differences are within the experimental uncertainties reported. This fact demonstrates that molar conductivity and diffusion coefficient presents the same temperature dependence for this family of ILs, at least in the temperature interval analysed.

In addition, we have calculated directly the values of Δ_{NE} in function of temperature for these two thiocyanate ILs. Results obtained appear in Table S6 and plots of the data in Fig. S5, both

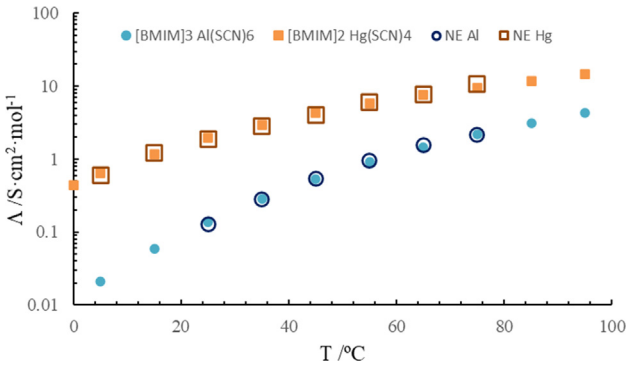

Fig. 7. Experimental molar conductivities, solid symbols, and calculated from Eqs. (6)–(8), open ones, for $[BMIM]_2$ $Hg(SCN)_4$ (dot symbols) and $[BMIM]_3$ $Al(SCN)_6$ (square symbols) versus temperature.

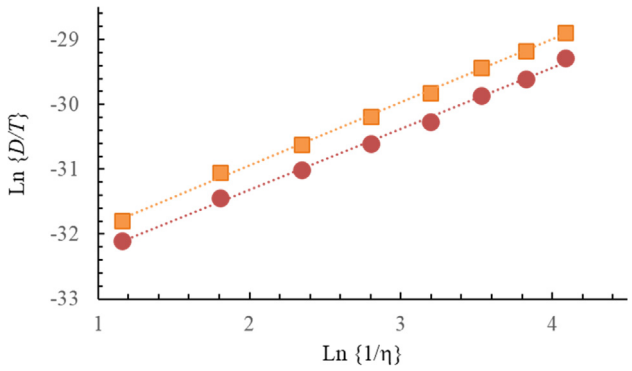

Fig. 8. Natural logarithm of diffusion constant divided by temperature versus that of fluidity for $[BMIM]_2$ $Hg(SCN)_4$ from 278 K to 348 K. Square symbols represent cations, D_B, and dot symbols the anionic complexes, D_M. The best fit of a straight line is shown. International System of Units has been used for all magnitudes.

in Supporting Information. As observed, value of this parameter is low at 0 °C for the compound with Hg, and it increases to about 0.35 at 40 °C, while above it is not dependent of temperature. With the IL with Al, we obtain a minimum in Δ_{NE} at about 15 °C, and then it increases up to values of 0.35 at 80 °C, at the highest temperatures studied the value of Δ_{NE} is equal for both compounds. So, we partially verify the low temperature dependence of this parameter as in [48], only for the sample with Hg and above 40 °C. Below that temperature Δ_{NE} decreases at rates higher than 0.01 per K. The sample with Al does not present any plateau for Δ_{NE} in the temperature interval studied, but its value seems to be constant above 80 °C.

4.3. Stokes-Einstein equation

We can relate the viscosity and diffusion coefficient through the Stokes-Einstein (SE) equation, which reads, for spherical ions [44]

$$D_i = \frac{k_B T}{6\pi\eta R_i} \tag{9}$$

If written in logarithmic form, and taking into account that in real concentrated electrolytes $D \propto {}^{T}/\eta^{t}$, the modified SE equation reads

$$Ln\left\{\frac{D}{T}\right\} = Ln\left\{\frac{k_B}{6\pi R_i}\right\} + t \cdot Ln\left\{\frac{1}{\eta}\right\} \tag{10}$$

where the factor t was introduced to correlate the theoretical expression with the experimental measurement in concentrate electrolytes as ILs (its meaning is equivalent to γ in Eq. (5)) [45]. In Fig. 8 we show this equation for $[BMIM]_2$ $Hg(SCN)_4$. We have taken as D_B for each of the two $[BMIM]^+$ cations from ^1H and ^{13}C NMR, and D_M for the $Hg(SCN)_4^{2-}$ anionic metallic complex, both with ^{13}C NMR spectra.

When plotting equation (10), as shown in Fig. 8, we observe a linear relationship between $Ln\{{}^{D}/_{T}\}$ and $Ln\{{}^{1}/\eta\}$ for the two diffusion coefficients measured, D_B (taken from ^{13}C spectra) and D_M. From the linear fit we observe that t = 0.97 for the cation and t = 0.94 for the anion, very near the ideal case with t = 1. The slopes from the Walden plot and from SE equation must be equal in absence of ion association [40], as mentioned above, γ for this compound is 0.93, very similar to that of the anionic complex. From the linear fit parameters obtained, we can calculate the hydrodynamic radio, R, of each compound, obtaining: 0.14 nm for the cation, 1.9 nm for the anionic complex and 3.3 nm for both ions together. These values are less than half than those obtained from volumetry presented before [1], but difference is obvious because in the previous calculus we took into account the empty space among ions, while here we have only the mobile entities.

We can define a theoretical SE diffusion constant, which would represent the average of both cations and anions,

$$D_{SE} = \frac{k_B T}{6\pi\eta r} \tag{11}$$

where we will use as IL effective molecular radio, r, that obtained from molar volume, calculated for these ILs in Ref. [1], which are 56.8 nm for the Hg compound and 64.4 nm for the Al one. Results obtained are included in Table 2, where we observe that are negative, indicating that D_{SE} values are lower than those measured, both for the cation and for the anionic complex. If we define a SE deviation parameter in analogy to Eq. (8), Δ_{SE}, we can calculate the decoupling parameter for diffusion,

$$D_{IL} = D_{SE}(1 - \Delta_{SE}) \tag{12}$$

To use this equation, we need a D_{IL} for the given compound comprising both anions. Using Fick's law and its analogy with the thermal equation [44,45], and assuming that $[BMIM]^+$ cation moves independently each other, while metallic anion moves as one entity, and that we have a parallel current of anions and cations, we can estimate this last quantity, D_{IL} as,

$$\frac{1}{D_{IL}} = \frac{n-z}{D_B} + \frac{1}{D_M} \tag{13}$$

Obtained Δ_{SE} parameter for the two analysed compounds is negative, which indicates that SE model underestimates the real value. Values are included in Table 2 at 25 °C, ranging from −0.05 for the sample with Zn, −0.10 for the reference sample up to −0.96 for the sample with Cu. In addition, we have calculated the temperature dependence of this deviation parameter for the samples with Al and Hg (where we have data of η and D vs. temperature). Results are included in Table S6 and data plotted in Figure S6, both in the Supporting Information section. As can be seen, while for the compound with Hg, the absolute value of Δ_{SE} is lower than 0.15, with a minimum at about 50 °C. In the case of the compound with Al, Δ_{SE} is about −1 at 0 °C and its absolute value decreases monotonically with increasing temperature up to −0.3 at 90 °C.

4.4. Laity's interionic friction coefficients

From the experimental data measured, we can obtain a new property, called interionic friction coefficient, r_{ij}, which is related to the total force per unit concentration of j that must be exerted on each mole of species i in order to maintain unit velocity of i relative to j [49]. Its inverse will be related with the conductivity of each ion in presence of the others of the same sign r_{++} or r_{--}, or dif-

ferent sign r_{+-} (due to reciprocity, $r_{+-} = r_{-+}$). This magnitude has not been widely used, but it has been applied by other authors to study conductivity in ionic liquids [46,50]. It reads,

$$r_{+-} = \frac{1}{e}\frac{(z_+ + z_-)F^2}{\Lambda} \tag{14}$$

$$r_{++} = \frac{1}{z_-}\left[\frac{(z_+ + z_-)RT}{D_+} - z_+ r_{+-}\right] \tag{15}$$

and,

$$r_{--} = \frac{1}{z_+}\left[\frac{(z_+ + z_-)RT}{D_-} - z_- r_{+-}\right] \tag{16}$$

where $z_+ = 1e$ and $z_- = (n\text{-}z)\cdot e$ for the different compounds, F is Faraday's constant, R is the gas constant and the rest of parameters have been defined above. Note that the number of cations in the chemical formula of any thiocyanate IL is not considered in Eqs. (14)–(16). Using the values measured for the molar conductance, Λ, and diffusion constant D given in Tables S1 and S3, we calculate the three friction coefficients for all samples for which D was measured. The values obtained for the three friction coefficients at 25 °C are given in Table 3.

As defined, the value of r_{+-} is inversely proportional to Λ, and so it does not give new relevant information. More interesting is the analysis of the values of r_{++} or r_{--} because they give information about the mobility of each ion. As expected, the r_{--} is much higher than r_{++} except for the reference sample. This indicates again that anion contribution to the overall conductivity is lower than that of the cation, being the coefficient r_{--}/r_{++} roughly the fraction of charge transported by each ion, their values are included in Table 3. Note that for $[BMIM]_3$ $Cu(SCN)_4$ coefficient r_{--}/r_{++} is around 2, the smallest among the metal thiocyanate ILs studied, indicating that the anion adduct has an important contribution to conductivity. This fact could explain the so relative high values of Δ_{NE} and Δ_{SE} respecting the other ILs (see Table 2). Finally, note that r_{--} for [BMIM](SCN) is negative, which is not unusual among molten salts and ionic liquids. This fact would indicate ion association [48–50], while for the other ILs it seems not to present ion pairing.

To know the temperature dependence of Laity interionic friction coefficients, we have calculated them for the samples $[BMIM]_2$ $Hg(SCN)_4$ and $[BMIM]_3$ $Al(SCN)_6$, and the data is plotted in Fig. 9. As observed r_{--} is much higher than r_{++} or r_{+-}, which have a similar value, indicating again that charge transport is primarily driven by the [BMIM] cation. Note that for the sample with Hg the value of r_{++} decreases faster with temperature than that of r_{+-}, crossing both values at approximately 23 °C. In Fig. 9 we plot VTF best fitting curves, while in Figure S7 we plot a Litovitz plot of the same data with the best fit of Eq. (2).

Table 3
Friction coefficients for some of the ILs studied at 25 °C: between anion and cation, r_{+-}, cation and cation, r_{++}, and anion and anion, r_{--}.

Compound	$r_{ij}\cdot 10^{10}$ in (J·s/cm²·mol)			
	r_{+-}	r_{++}	r_{--}	r_{--}/r_{++}
[BMIM] (SCN)	1.43	1.67	−0.16	−0.09
$[BMIM]_2Hg(SCN)_4$	1.43	1.51	4.53	3.01
$[BMIM]_2Zn(SCN)_4$	2.38	1.92	11.8	6.16
$[BMIM]_3Cu(SCN)_4$	3.57	3.23	6.16	1.91
$[BMIM]_3$ $Al(SCN)_6$	27.1	24.9	442	17.8

4.5. Theoretical considerations

Data obtained for transport properties for these new ILs must not be explained using the classical models given by Nernst-Einstein (NE) and Stokes-Einstein (SE) equations, where it is assumed that cations and anions are completely independent each other, moving the charge carriers in a continuous path by diffusion. The nanostructure of the ILs, which are molten salts without solvent, are in the opposite side of the diluted electrolyte described for those models. In our case, we have the electrolyte formed by only $[BMIM]^+$ cations and anionic metal thiocyanate adducts $[M(SCN)n]^{-(n-z)}$ (being n the number of thiocyanate anions in the complex and z the metal valency). Both entities are more or less bonded by intraionic forces depending on the compound. Although the three transport properties measured (ionic conductivity, viscosity and diffusion constant) follow the relationships given by the NE and SE models (with the corresponding deviation parameter Δ_{SE} and Δ_{NE}). This fact indicates that the three properties are related among them somehow, apart from following the same temperature behaviour (VTF equation (1) and Litovitz equation (2)).

To explain the data obtained, we will use the recently developed pseudolattice model for conduction in electrolytes [51,52]. It is valid in all range of concentrations, up to saturated electrolytes and so suitable for ILs. This theoretical model propose that ions move using a hopping mechanism through a pseudo-lattice net formed by anions and cations. Thus, each ion simply hops from an ionic aggregate to an adjacent one, being confined there for a given time. This hopping mechanism, similar to the Grotthuss one for protons, would be also the origin of the diffusion constant measured, and it must also be related with fluidity, where movement of each individual ion would be by hops instead by a continuous diffusive mechanism. Hopping mechanisms of charge and mass transport, completely different than for classical models, could also explain the apparent superionic behaviour of the stud-

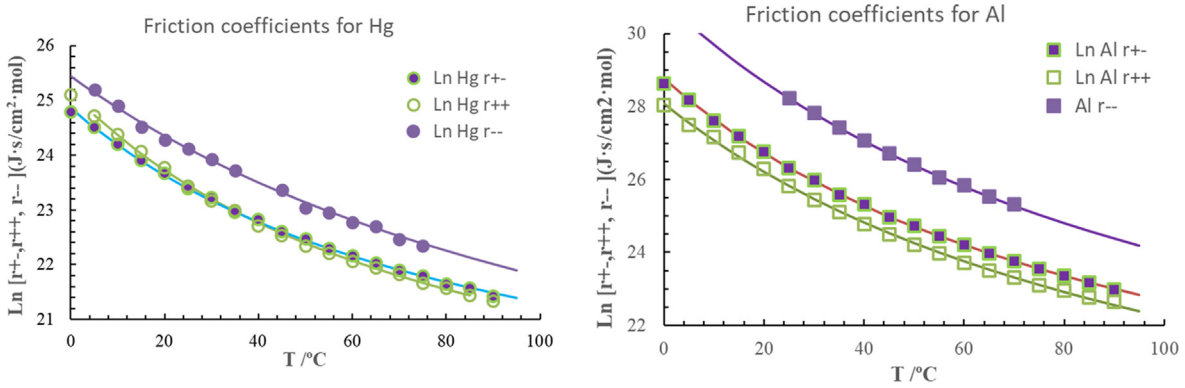

Fig. 9. Semi-Arrhenius plot of the temperature dependence of Laity interionic friction coefficients, where solid symbols correspond to r_{--}, open symbols to r_{++} while doted ones to r_{+-}. At left for $[BMIM]_2$ $Hg(SCN)_4$ (dot symbols) and at right for $[BMIM]_3$ $Al(SCN)_6$ (square symbols). with the VTF best fitting equations shown.

ied ILs, including all conducting ionogels (which present ionic conductivity but no fluidity) [43,53]. This Grotthuss-like ion hopping mechanism of conduction has been already proposed to explain transport data measured in some ILs and semisolid conductors [33,34,53]. It could be the clue to develop a theoretical model capable of explaining observed transport properties with hopping mechanism in a pseudo-lattice model, which is one of our aims.

If we compare the properties measured for the studied novel ILs, we observe that the mobility of cations and thiocyanate metal complexes studied for the three transport properties is coherent for each IL, but they are very different among the compounds. The metal cation nature seems not to explain the results measured, due to the lack of periodicity of these with the mass, size, ionic surface charge or electrical potential at the surface of the different metal atoms, as observed in Table 2. In contrast, it is observed that values measured order scale with the first row of transition metals in the periodic table (except for the magnetic nuclei as Fe or Ni), which implies that the electronic quantum configuration of the metal nuclei affect the stability of the adduct formed, which is related with the bonding strength between thiocyanate anions and metal cations in every IL. Thus, although tetrahedral configuration has in general highest values of molar conductivity, fluidity and diffusion constant than octahedral ones, this fact does not happen in all cases. In addition, due to the size and weight of the metal thiocyanate adducts, it would be expected to have very low diffusion constant compared to that of $[BMIM]^+$ cation, it is the case, having higher value D for the cation than for the anion (except for the reference sample because here cation is greater than anion). The calculation of interionic friction coefficient will emphaticise this fact, observing that for both extremal compounds analysed, friction among anions is much higher than that among cations, which reinforce the idea that are majority cations the responsible for charge transport through a hopping mechanism in a pseudolattice ionic network.

5. Conclusions

We have measured three transport properties in a set of 10 ionic liquid compounds, being majority of data never published before at our knowledge, in a wide temperature range: ionic (or electrical) conductivity, κ, viscosity, η, and diffusion coefficient, D. The ILs studied are based in the popular 1-butyl-3-methyl imidazolium cation, $[BMIM]^+$, with a metal thiocyanate complex anion. Apart from the reference sample, [BMIM](SCN), we have measured ionic conductivity in metallic thiocyanates with Al, Mn, Fe, Cr, Ni, Hg, Zn, Co and Cu as metal cations, while viscosity was measured in five of them and diffusion coefficient in five compounds also. The formed adducts between the metal cation and the (SCN) anions form octahedral (for the 5 first metals) or tetrahedral (for the last four) configurations. Values obtained for the three properties measured exhibit differences of more than one order of magnitude among the different compounds. By using density data published for these compounds, we calculated the molar conductivity, Λ. The three transport properties have a Vogel-Tamman-Fulcher and Litovitz's $1/T^3$ exponential temperature behaviour, and the best fits are included. Also, the three have been compared in pairs employing classical theoretical models: Walden's rule (for Λ and η), Stokes-Einstein (for η and D), Nerst-Einstein (for Λ and D) and we have extracted interionic friction coefficient of both anions for two selected samples. A great coherence among the three properties for each of the different samples was found, being the three models (modified for saturated electrolytes) followed by the data for each sample. We explain qualitatively the evidences obtained using a pseudo-lattice model, which implies an ionic movement by a Grotthuss-like hopping mechanism of ions, instead the classical diffusion one. Finally, we find that values measured scale with the first row of transition metals in the periodic table (except for the magnetic nuclei as Fe or Ni), which implies that the electronic quantum configuration of the metal nuclei affects the stability of the adduct formed, which is related with the bonding strength between anions and cations in every IL.

CRediT authorship contribution statement

Oscar Cabeza: Conceptualization, Formal analysis, Investigation, Writing – original draft, Supervision, Project administration, Funding acquisition. **Luisa Segade:** Formal analysis, Writing – review & editing, Visualization. **Montserrat Domínguez-Pérez:** Resources, Data curation, Writing – review & editing. **Esther Rilo:** Validation, Formal analysis. **David Ausín:** Investigation, Data curation. **Julio A. Seijas:** Conceptualization, Investigation, Writing – review & editing. **M. Pilar Vazquez-Tato:** Validation, Investigation, Resources. **Vladimir Matleev:** Conceptualization, Writing – review & editing. **Alexandr Ievlev:** Validation, Formal analysis, Investigation, Resources. **Josefa Salgado:** Validation, Resources. **Luis M. Varela:** Conceptualization, Writing – review & editing, Supervision, Project administration, Funding acquisition.

Declaration of Competing Interest

The authors declare that they have no known competing financial interests or personal relationships that could have appeared to influence the work reported in this paper.

Acknowledgements

We acknowledge the fine measurements performed by the UDC technician M. Cabanas. We also acknowledge the financial support of Ministerio de Economía y Competitividad MINECO) (MAT2017-86109-P and MAT2017-89239-C2-(1.2)-P); and Xunta de Galicia (AGRU 015/11. GRC ED431C 2016/001 and ED431D 2017/06). All these research projects were partially supported by FEDER. Also, D.A. acknowledges Gil Dávila Foundation for his postgraduate grant. Funding for open access charge: Universidade da Coruña/CISUG.

Appendix A. Supplementary data

Supplementary data to this article can be found online at https://doi.org/10.1016/j.molliq.2021.117164.

References

[1] O. Cabeza, Luis M. Varela, Esther Rilo, Luisa Segade, Montserrat Domínguez-Pérez, David Ausín, Manuel de Pedro, Jesús Rodríguez Fernández, Jesus Gonzalez, M. Pilar Vázquez-Tato, Yago Arosa, Elena Lopez Lago, Raul De la Fuente, Juan Jose parajo, Josefa Salgado, Maria Villanueva, Vladimir Matveev, Alexandr Ievlev, Julio A. Seijas. Synthesis, microstructure and volumetry of novel metal thiocyanate ionic liquids with BMIM cation. J. Mol. Liq. 283 (2019) 638–651.

[2] M.M. Vadiyar, S.K. Patil, S.C. Bhise, A.V. Ghule, S.-H. Han, S.S. Kolekar, Improved electrochemical performance of a $ZnFe_2O_4$ nanoflake-based supercapacitor electrode by using thiocyanate-functionalized ionic liquid electrolytes, Eur. J. Inorg. Chem. 2015 (36) (2015) 5832–5838.

[3] Z.P. Rosol, N.J. German, S.M. Gross, Solubility, ionic conductivity and viscosity of lithium salts in room temperature ionic liquids, Green Chem. 11 (2009) 1453–1457.

[4] S.A. Dharaskar, K.L. Wasewar, M.N. Varma, D.Z. Shende, Synthesis, characterization, and application of 1-butyl-3-methylimidazolium thiocyanate for extractive desulfurization of liquid fuel, Environ. Sci. Pollut. Res. 23 (2016) 9284–9294.

[5] M. Larriba, P. Navarro, J. Garcia, F. Rodriguez, Selective extraction of toluene from n-heptane using [emim][SCN] and [bmim][SCN] ionic liquids as solvents, J. Chem. Thermodyn. 79 (2014) 266–271.

[6] R.D. Rogers, K.R. Seddon (Eds.), Ionic Liquids, Industrial Applications to Green Chemistry, ACS Symp. Series 818, Am. Chem. Soc., Washington, 2002.

[7] D.R. Macfarlane, M. Kar, J.M. Pringle. Physical and thermal properties, in: Fundamentals of Ionic Liquids From Chemistry to Applications. Wiley and Sons, 2017, pp. 103–142.
[8] G. Gonfa, M.A. Bustam, N. Muhammad, A.S. Khan, Evaluation of thermophysical properties of functionalized imidazolium thiocyanate based ionic liquids, Ind. Eng. Chem. Res. 54 (2015) 12428–12437.
[9] C.M.S.S. Neves, K.A. Kurnia, J.A.P. Coutinho, I.M. Marrucho, J.N.C. Lopes, M.G. Freire, L.P.N. Rebelo, Systematic study of the thermophysical properties of imidazolium- based ionic liquids with cyano-functionalized anions, J. Phys. Chem. B 117 (2013) 10271–10283.
[10] G. Vakili-Nezhaad, M. Vatani, M. Asghari, I. Ashour, Effect of temperature on the physical properties of 1-butyl-3-methylimidazolium based ionic liquids with thiocyanate and tetrafluoroborate anions, and 1-hexyl-3-methylimidazolium with tetrafluoroborate and hexafluorophosphate anions, J. Chem. Thermodynamics 54 (2012) 148–154.
[11] S.A. Pandit, M.A. Rather, S.A. Bhat, G.M. Rather, M.A. Bhat, Influence of the anion on the equilibrium and transport properties of 1-butyl-3-methylimidazolium based room temperature ionic liquids, J Solution Chem. 45 (2016) 1641–1658.
[12] U. Domanska, M. Królikowska, Density and viscosity of binary mixtures of thiocyanate ionic liquids + water as a function of temperature, J. Solution Chem. 41 (2012) 1422–1445.
[13] U. Domańska, M. Laskowska, Temperature and composition dependence of the density and viscosity of binary mixtures of {1-butyl-3-methylimidazolium thiocyanate + 1-alcohols}, J. Chem. Eng. Data 54 (7) (2009) 2113–2119.
[14] U. Domańska, M. Królikowska, Density and viscosity of binary mixtures of {1-butyl-3-methylimidazolium thiocyanate + 1-heptanol, 1-octanol, 1-nonanol, or 1-decanol}, J. Chem. Eng. Data 55 (9) (2010) 2994–3004.
[15] M.L.S. Batista, L.I.N. Tome, C.M.S.S. Neves, J.R.B. Gomes, J.A.P. Coutinho, Characterization of systems of thiophene and benzene with ionic liquids, J. Mol. Liq. 192 (2014) 26–31.
[16] H.F.D. Almeida, J.N. Canongia Lopes, L.P.N. Rebelo, J.A.P. Coutinho, M.G. Freire, I.M. Marrucho, Densities and viscosities of mixtures of two ionic liquids containing a common cation, J. Chem. Eng. Data 61 (2016) 2828–2843.
[17] A. Mondal, S. Balasubramanian, A refined all-atom potential for imidazolium-based room temperature ionic liquids: acetate, dicyanamide, and thiocyanate anions, J. Phys. Chem. B 119 (2015) 11041–11051.
[18] S.J. Osborne, S. Wellens, C. Ward, S. Felton, R.M. Bowman, K. Binnemans, M. Swadźba-Kwaśny, H.Q.N. Gunaratnea, P. Nockemann, Thermochromism and switchable paramagnetism of cobalt(II) in thiocyanate ionic liquids, Dalton Trans. 44 (2015) 11286–11289.
[19] B. May, M. Hönle, B. Heller, F. Greco, R. Bhuin, H.-P. Steinrück, F. Maier, Surface-induced changes in the thermochromic transformation of an ionic liquid cobalt thiocyanate complex, J. Phys. Chem. Lett. 8 (2017) 1137–1141.
[20] Z. Wang, L. Wang, Y. Zhang, J. Guo, H. Li, F. Yan, Dye-sensitized solar cells based on cobalt containing room temperature ionic liquid redox shuttles, RSC Adv. 7 (2017) 13689–13695.
[21] E. López Lago, J.A. Seijas, I. de Pedro, J. Rodríguez Fernández, M.P. Vázquez-Tato, J.A. González, E. Rilo, L. Segade, O. Cabeza, C.D. Rodríguez Fernández, Y. Arosa, B.S. Algnamat, L.M. Varela, J. Troncoso, R. de la Fuente, Structural and physical properties of a new reversible and continuous thermochromic ionic liquid in a wide temperature interval: $BMIM_4Ni(NCS)_6$, New J. Chem. 42 (19) (2018) 15561–15571.
[22] A.D. Santo, H. Pérez, G.A. Echeverría, O.E. Piro, R.A. Iglesias, R.E. Carbonio, A.B. Altabet, D.M. Gil, Exploring weak intermolecular interactions in thiocyanate-bonded Zn(II) and Cd(II) complexes with methylimidazole: crystal structures, Hirshfeld surface analysis and luminiscence properties, RSC Adv. 8 (2018) 23891–23902.
[23] J.A. Nóvoa-López, E. López-Lago, J.A. Seijas, M.P. Vázquez-Tato, J. Troncoso, R. de la Fuente, J.R. Salgueiro, H. Michinel, Nonlinear absorption in ionic liquids with transition metallic atoms in the anion, Optical Mater. 52 (2016) 144–149.
[24] A.E. Phillips, A.L. Goodwin, G.J. Halder, P.D. Southon, C.J. Kepert, Nanoporosity and exceptional negative thermal expansion in single-network cadmium cyanide, Angew. Chem. Int. Ed. 47 (2008) 1396–1399.
[25] A.L. Goodwin, M. Calleja, M.J. Conterio, M.T. Dove, J.S.O. Evans, D.A. Keen, L. Peters, M.G. Tucker, Colossal positive and negative thermal expansion in the framework material $Ag_3[Co(CN)_6]$, Science 319 (2008) 794–797.
[26] H. Vogel, The law of the relationship between viscosity of liquids and the temperature, Phys. Z. 22 (1921) 645.
[27] G.S. Fulcher, Analysis of recent measurements of the viscosity of glasses, J. Am. Ceram. Soc. 8 (1952) 339.
[28] G. Tammam, W. Hesse, Die Abhängigkeit der viscosität von der temperatur bie unterkühlten flüssigkeiten, Z. Anorg. Allg. Chem. 156 (1926) 245.
[29] J. Vila, P. Ginés, J.M. Pico, C. Franjo, E. Jiménez, L.M. Varela, O. Cabeza, Temperatura dependence of electrical conductivity in EMIM-based ionic liquids. Evidence of Vogel-Tamman-Fulcher behavior, Fluid Phase Equilib. 242 (2006) 141–146.
[30] T.A. Litovitz, Temperature dependence of viscosity in associated liquids, J. Chem. Phys. 20 (1952) 1088–1089.
[31] M. Kanakubo, K.R. Harris, N. Tsuchihashi, K. Ibuki, M. Ueno, Temperature and pressure dependence of the electrical conductivity of the ionic liquids 1-methyl-3-octylimidazolium hexafluorophosphate and 1-methyl-3-octylimidazolium tetrafluoroborate, Fluid Phase Equilib. 261 (1-2) (2007) 414–420.
[32] A.I. Komayko, E.A. Arkhipova, A.S. Ivanov, K.I. Maslakov, S.Y. Kupreenko, H. Xia, S.V. Savilov, V.V. Lunin, Conductivity of N-(2-methoxyethyl)-substituted morpholinium- and piperidinium-based ionic liquids and their acetonitrile solutions, Funct. Mater. Lett. 11 (2018) 1840009.
[33] E.A. Arkhipova, A.S. Ivanov, K.I. Maslakov, S.V. Savilov, V.V. Lunin, Effect of cation structure of tetraalkylammonium- and imidazolium-based ionic liquids on their conductivity, Electrochim. Acta 297 (2019) 842–849.
[34] S. García-Garabal, J. Vila, E. Rilo, M. Domínguez-Pérez, L. Segade, E. Tojo, P. Verdía, L.M. Varela, O. Cabeza, Transport properties for 1-ethyl-3-methylimidazolium n-alkyl sulfates: possible evidence of Grotthuss mechanism, Electrochim. Acta 231 (2017) 94–102.
[35] R.D. Shannon, Revised effective ionic radii and systematic studies of interatomic distances in halides and chalcogenides, Acta Cryst. A 32 (5) (1976) 751–767.
[36] K.R. Harris, M. Kanakubo, L.A. Woolf, Temperature and Pressure Dependence of the Viscosity of the Ionic Liquid 1-Butyl-3-methylimidazolium Tetrafluoroborate: Viscosity and Density Relationships in Ionic Liquids, J. Chem. Eng. Data 52 (2007) 2425–2430.
[37] W. Xu, E.I. Cooper, C.A. Angell, Ionic liquids: ion mobilities, glass temperatures, and fragilities, J. Phys. Chem. B 107 (2003) 6170.
[38] D.R. MacFarlane, M. Forsyth, E.I. Izgorodina, A.P. Abbott, G. Annat, K. Fraser, On the concept of ionicity in ionic liquids, Phys. Chem. Chem. Phys. 11 (25) (2009) 4962, https://doi.org/10.1039/b900201d.
[39] K. Ueno, H. Tokuda, M. Watanabe, Ionicity in ionic liquids: correlation with ionic structure and physicochemical properties, Phys. Chem. Chem. Phys. 12 (2010) 1649–1658.
[40] S. Bulut, P. Eiden, W. Beichel, J.M. Slattery, T.F. Beyersdorff, T.J.S. Schubert, I. Krossing, Temperature dependence of the viscosity and conductivity of mildly functionalized and non-functionalized $[Tf_2N]^-$ ionic liquids, ChemPhysChem 12 (2011) 2296–2310.
[41] C. Schreiner, S. Zugmann, R. Hartl, H.J. Gores, Fractional Walden rule for ionic liquids: examples from recent measurements and critique of the so-called ideal KCl line for the Walden plot, J. Chem. Eng. Data 55 (2010) 1784–1788.
[42] H. Liu, E. Maginn, An MD study of the applicability of the Walden rule and the Nernst-Einstein model for ionic liquids, ChemPhysChem 13 (7) (2012) 1701–1707.
[43] O. Cabeza, L. Segade, M. Domínguez-Pérez, E. Rilo, S. García-Garabal, D. Ausín, A. Martinelli, E. López-Lago, L.M. Varela, Tuning physical properties and mesomorphic structures in aqueous 1-ethyl-3-methylimidazolium octylsulfate rigid-gel with univalent salt doping, J. Chem. Thermodynamics 112 (2017) 267–275.
[44] J.O'M. Bockris, A.K.N. Reddy, in: Modern Electrochemistry, Springer US, Boston, MA, 1970, pp. 1–44, https://doi.org/10.1007/978-1-4615-7464-4_1.
[45] K.R. Harris, Relations between the fractional Stokes-Einstein and Nernst-Einstein equations and velocity correlation coefficients in ionic liquids and molten salts, J. Phys. Chem. B 114 (29) (2010) 9572–9577.
[46] T. Rüther, K.R. Harris, M.D. Horne, M. Kanakubo, T. Rodopoulos, J.-P. Veder, L.A. Woolf, Transport, electrochemical and thermophysical properties of two N-donor-functionalised ionic liquids, Chem. Eur. J. 19 (2013) 17733–17744.
[47] J.P. Hansen, I.R. McDonald, Statistical mechanics of dense ionized matter. IV. Density and charge fluctuations in a simple molten salt, Phys. Rev. A 11 (1975) 2111–2123.
[48] K.R. Harris, Can the transport properties of molten salts and ionic liquids be used to determine ion association?, Phys Chem. B 120 (47) (2016) 12135–12147.
[49] R.W. Laity, Interionic friction coefficients in molten salts, Ann. New York Acad. Sci. 79 (1960) 997–1022.
[50] K.R. Harris, M. Kanakubo, Revised and extended values for self-diffusion coefficients of 1-alkyl-3-methylimidazolium tetrafluoroborates and hexafluorophosphates: relations between the transport properties, J. Phys. Chem. B 120 (2016) 12937–12949.
[51] L.M. Varela, J. Carrete, M. García, J.R. Rodríguez, M. Turmine, O. Cabeza, Pseudolattice theory of ionic liquids, in: A. Kokorin (Ed.), Ionic Liquids: Theory, properties, new approaches, In Tech, pp. 347–366, Wien 2011, ISBN: 978-953-307-349-1.
[52] H. Montes-Campos, S. Kondrat, E. Rilo, O. Cabeza, L.M. Varela, Random-alloy Model for the Conductivity of Ionic Liquid-Solvent Mixtures, J. Phys. Chem. C 124 (2020) 11754–11759.
[53] O. Cabeza, E. Rilo, L. Segade, M. Domínguez-Pérez, S. García-Garabal, D. Ausín, E. López-Lago, L.M. Varela, M. Vilas, P. Verdía, E. Tojo, Imidazolium decyl sulfate: a very promising selfmade ionic hydrogel, Mat. Chem. Frontiers 2 (2018) 505–513.